remote sensing

MDPI

Article

Spatiotemporal Evolution of Arid Ecosystems Using Thematic Land Cover Products

Lili Xu [1,2,*], Tianyu Chen [1], Baolin Li [3], Yecheng Yuan [3] and Nandin-Erdene Tsendbazar [4]

[1] College of Urban and Environmental Sciences, Central China Normal University, Wuhan 430079, China
[2] Key Laboratory for Geographical Process Analysis & Simulation of Hubei Province, Central China Normal University, Wuhan 430079, China
[3] State Key Laboratory of Resources and Environmental Information System, Institute of Geographic Sciences and Natural Resources Research, Beijing 100101, China
[4] Laboratory of Geo-Information Science and Remote Sensing, Wageningen University & Research, Droevendaalsesteeg 3, 6708 PB Wageningen, The Netherlands
* Correspondence: xulls@mail.ccnu.edu.cn

Abstract: The pathway, direction, and potential drivers of the evolution in global arid ecosystems are of importance for maintaining the stability and sustainability of the global ecosystem. Based on the Climate Change Initiative Land Cover dataset (CCILC), in this study, four indicators of land cover change (LCC) were calculated, i.e., regional change intensity (*RCI*), rate of change in land cover (*CR*), evolutionary direction index (EDI), and artificial change percentage (ACP), to progressively derive the intensity, rate, evolutionary direction, and anthropogenic interferences of global arid ecosystems. The LCC from 1992 to 2020 and from 28 consecutive pair-years was observed at the global, continental, and country scales to examine spatiotemporal evolution in the Earth's arid ecosystems. The following main results were obtained: (1) Global arid ecosystems experienced positive evolution despite complex LCCs and anthropogenic interferences. Cautious steps to avoid potential issues caused by rapid urbanization and farmland expansion are necessary. (2) The arid ecosystems in Australia, Central Asia, and southeastern Africa generally improved, as indicated by *EDI* values, but those in North America were degraded, with 41.1% of LCCs associated with urbanization or farming. The arid ecosystems in South America also deteriorated, but 83.4% of LCCs were in natural land covers. The arid ecosystems in Europe slightly improved with overall equivalent changes in natural and artificial land covers. (3) Global arid ecosystems experienced three phases of change based on *RCI* values: 'intense' (1992–1998), 'stable' (1998–2014), and 'intense' (2014–2020). In addition, two phases of evolution based on *EDI* values were observed: 'deterioration' (1992–2002) and 'improvement' (2002–2020). The ACP values indicated that urbanization and farming activities contributed increasingly less to global dryland change since 1992. These findings provide critical insights into the evolution of global arid ecosystems based on analyses of LCCs and will be beneficial for sustainable development of arid ecosystems worldwide within the context of ongoing climate change.

Keywords: global dryland; land cover change; CCILC; remote sensing; multi-indices classifiers; sustainable global ecosystems

Citation: Xu, L.; Chen, T.; Li, B.; Yuan, Y.; Tsendbazar, N.-E. Spatiotemporal Evolution of Arid Ecosystems Using Thematic Land Cover Products. *Remote Sens.* **2023**, *15*, 3178. https://doi.org/10.3390/rs15123178

Academic Editors: Hossein Shafizadeh-Moghadam, Jay Gao and Tingting Xu

Received: 4 April 2023
Revised: 12 June 2023
Accepted: 16 June 2023
Published: 19 June 2023

1. Introduction

Arid ecosystems are habitats for dryland flora and fauna, playing an essential role in supporting terrestrial carbon sinks and biodiversity at a global scale [1,2]. The evolution of arid ecosystems influences cycling processes of the hydrosphere, atmosphere, and biosphere [3–5] and is of importance for the stability and sustainability of the global ecosystem.

However, arid ecosystems are usually fragile [6]. The evolution of arid ecosystems is influenced by external interferences [7–9], such as climate change [10–12] and human activities [13–15]. Global warming is generally now acknowledged based on diverse sources of

evidence [16–18]. The global area of drylands is expanding, and drylands are predicted to face greater stress than non-drylands in response to ongoing global warming [19]. Human societies in drylands worldwide are experiencing unprecedented change. Increasing urbanization and farming practices are reshaping arid ecosystems in direct and indirect ways [20,21]. Within the context of recent global warming and economic globalization, close observation and a rich understanding of evolution in global arid ecosystems are essential for maintaining and improving the resistance and resilience of these unique areas in response to future unprecedented interferences.

Land cover change (LCC), an indicator of the modifications of the Earth's surface [22], could provide a framework to interpret the evolutionary processes of Earth's ecosystems. Previous research linked LCCs with several aspects of ecosystems, for instance, ecosystem services [23], resilience [24], and biodiversity [25]. The transitions among land covers may indicate the evolutionary behavior of ecosystems [26,27]. Changes in specific land covers provide clues to natural or anthropogenic drivers of ecological evolution [28,29]. Thus, monitoring LCC in global drylands is a practical and effective means to understand the pathway, direction, and potential drivers of the evolution of global arid ecosystems.

Remote sensing platforms, such as AVHRR, MODIS, and Landsat [30–32], are efficient for monitoring LCC at local [20,33], regional [34], and global scales [35–38]. Although previous studies have used time-series vegetation indices to capture the land surface change in global drylands [39–41], few studies have focused on the long-term evolution of Earth's ecosystems from the perspective of LCC. A few studies have investigated the land cover dynamics in dry areas, but such studies focused on limited areas of drylands [13,42] or a selected thematic LCC [43]. Specifically, Central Asia [44], China [45], southeastern Australia [46], and southeastern Africa [47] have experienced the loss of bare land and overall greening in vegetation, whereas the arid ecosystems in South America have been degraded [48]. Meanwhile, wetland shrinkage has been documented in Uzbekistan [49]. These accounts present different conclusions and differ in study periods, and hence discerning spatiotemporal changes in global drylands is difficult [34,50]. To date, it is unclear whether certain dryland hotspots with striking LCCs are representative of drylands worldwide, as well as whether global arid ecosystems evolve in a linear or nonlinear manner in the long term. Several global studies of thematic LCCs have recorded a decrease in the area of bare land [36,37], an increase in water-body area [51,52], net loss of forests and grasslands [36,37], and rapid expansion of urban areas and agricultural land [36,53]. However, the performance of thematic LCCs in relation to global drylands, compared with that for global non-drylands, remains unknown. Elucidation of the evolutionary processes in arid ecosystems worldwide remains a challenging task.

The scientific question posed in the present study was as follows: what are the unique spatiotemporal evolutionary processes of Earth's arid ecosystems, within the context of global warming and economic globalization? To answer this question, long-term LCCs in drylands at global, continental, and country scales were determined using the Climate Change Initiative Land Cover (CCILC) dataset (1992–2020). Four indicators, i.e., regional change in intensity of land cover (*RCI*), rate of change in land cover (*CR*), evolutionary direction index (EDI), and artificial change percentage (ACP), were used to derive the intensity, rate, evolutionary direction, and anthropogenic interferences of global arid ecosystems based on the LCCs. We first determined the evolutionary characteristics of global drylands from 1992 to 2020, and then derived the evolutionary processes in 28 consecutive pair-years. In this manner, we interpreted the diversity and uniqueness of evolution in global drylands, as well as the nonlinear evolutionary paths of global arid ecosystems. The present research provides fundamental evidence of how global drylands have changed and how arid ecosystems have evolved during the past three decades. The findings are of importance for understanding the evolutionary mechanism of worldwide arid ecosystems from the perspective of LCCs.

2. Methods

2.1. Study Area

The extent of global drylands was determined based on the global climate map using the Köppen–Geiger system and downloaded from the Global Groundwater Information System website (https://ggis.un-igrac.org/catalogue/#/dataset/431 (accessed on 4 May 2023)). The most recent version of the map was released in October 2020. The Köppen–Geiger system includes five climate zones of global extent. The five zones, i.e., tropical (A), arid (B), temperate (C), continental (D), and polar (E), were determined by consideration of the local vegetation, long-term precipitation, and long-term temperature status [54]. In the present study, the dryland area refers to the arid zone (B) of the Köppen–Geiger system, covering four subzones, i.e., the BWh area (Arid-Desert-Hot), BWk area (Arid-Desert-Cold), BSh area (Arid-Steppe-Hot), and BSk area (Arid-Steppe-Cold).

The study area was generally located between 10° and 50° N/S and covered 97 countries (Figure S1). Given that 35 of the 97 countries had dryland areas of less than 0.02 million km^2, these countries (0.35% of the global dryland area) were excluded from the analysis. Ultimately, the study area included 62 countries on six continents and covered 41.14 million km^2 in total (Table S1).

2.2. Data

The CCILC dataset has been widely used in previous LCC monitoring studies [20,36,55] and was downloaded from the official website of the European Space Agency (https://www.esa-landcover-cci.org (accessed on 25 June 2022)). The dataset contains annual land-cover maps from 1992 to 2020 with 300 m spatial resolution and using the WGS84 geographic coordinate system. The dataset was produced using the Advanced Very High-Resolution Radiometer (AVHRR) time series (1992–1999), the Systeme Probatoire d'Observation de la Terre Vegetation (SPOT-VGT) time series (1999–2013), the Project for On-Board Autonomy V (Proba-V) time series (2014–2015), and the Sential-3 Ocean Land Color Instrument (S3-OLCI) time series (2016–2020). The overall accuracy of the land-cover map in the year 2015 proved to be 71.45% in comparison with the GlobCover 2009 validation database [56].

The 37 land-cover categories in the dataset were determined using the Land Cover Classification System (LCCS), which was developed by the Food and Agriculture Organization of the United Nations. Based on the description of the individual land-cover categories, the 37 land-cover categories were regrouped into eight categories, i.e., farmland, forest, grassland, wetland, urban land, shrubland, bare land, and other lands, with consideration of the land cover/land use definitions in the Intergovernmental Panel on Climate Change land classification system, as well as the ecological function and ecosystem service of each land-cover category (Table S2).

2.3. Land Cover Change Indices

In this study, the CCILC dataset was the only data source. Four indicators (*RCI*, *CR*, EDI, and ACP) were calculated to progressively capture the intensity, rate, evolutionary direction, and potential anthropogenic contributions of the LCCs in global drylands. The statistical computing was conducted using the C# language with ArcGIS Engine functions.

In theory, all indices could be derived by comparing land-cover maps from two specific years. We first calculated the four indices using the land-cover maps for 1992 and 2020 to outline the long-term changes. Then, we calculated *RCI*, EDI, and ACP in 28 consecutive pair-years to enrich information on the detailed pathway of the changes (Figure 1). In this manner, the long-term consequences and the tortuous evolutionary paths of global arid ecosystems were considered. A pair-year refers to two consecutive years starting from 1992, for instance, 1992–1993, 1993–1994, and so forth. As a result, there were 29 years and 28 pair-years. The pair-year results were recorded using the start year. For example, the *EDI* of 1992 denotes the *EDI* calculated using the land cover maps in 1992 and 1993. All maps were visualized using ArcGIS 10.5 software.

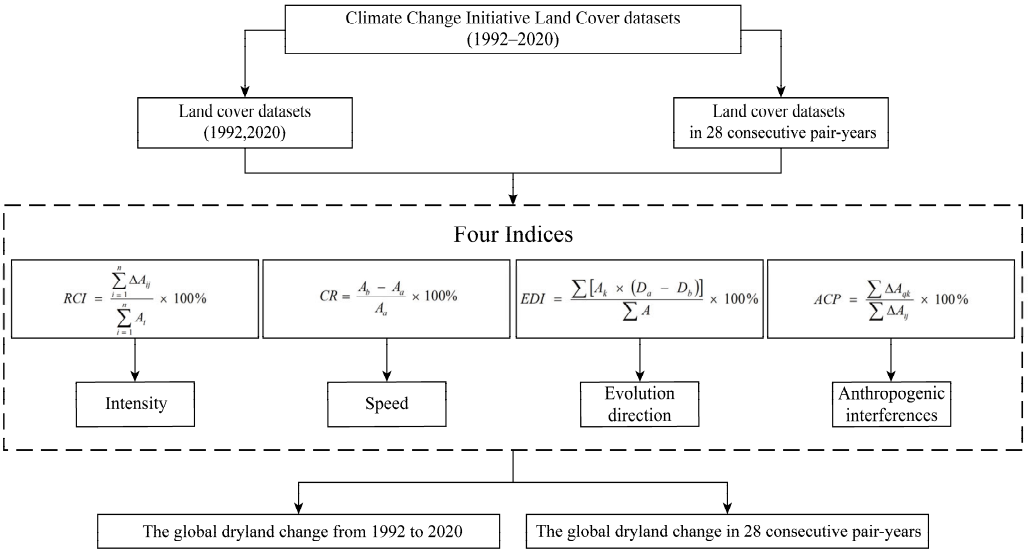

Figure 1. The workflow of this study.

- Regional change intensity (*RCI*)

The *RCI* is a comprehensive indicator of the intensity of LCCs within a specific spatial extent for two specific years [57]. It considers all potential transitions among land-cover categories and was calculated using Equation (1). The *RCI* is always a positive value. A high *RCI* value indicates a high intensity of LCCs for a given area.

$$RCI = \frac{\sum_{i=1}^{n} \Delta A_{ij}}{\sum_{i=1}^{n} A_i} \times 100\% \quad (1)$$

where A_i is the area of land-cover category i in the start year, and ΔA_{ij} is the absolute change in areas in which land-cover category i was transferred to category j. Note that i and j are two different land-cover categories.

- Rate of change in land cover (*CR*)

The *CR* indicates the rate of change of land cover categories within a specific spatial extent for two given years [57,58]. The *CR* was calculated using Equation (2):

$$CR = \frac{A_b - A_a}{A_a} \times 100\% \quad (2)$$

where A_a and A_b are the area of a specific land-cover category in year a and year b, respectively.

- Evolutionary direction index (*EDI*)

The *EDI* was conceived to indicate the direction of ecological evolution owing to LCCs [58]. Because different land cover categories indicate various ecological functions and values [59,60], we assigned levels 1 to 5 to each of the eight land-cover categories to represent their influence on ecosystems (Table 1). The ecological levels of the different land-cover categories were assigned in accordance with previous studies [58,61]. A lower ecological level indicates a higher benefit to an ecosystem (Table 1). Based on the equivalent value per unit area of ecosystem services determined in a previous study [60], we determined wetland (including water bodies and lakes) as having the highest ecological level (i.e., 1).

Table 1. Ecological level assigned to each land-cover category.

Land Cover	Farmland	Forest	Grassland	Wetland	Urban Area	Shrub	Bare	Others
Ecological level	5	2	4	1	5	3	5	5

The *EDI* is a comprehensive indicator. Every local land-cover transition among the eight categories contributes to the *EDI* value. The direction of ecological evolution at a specific site was determined by comparison of ecological levels over two years. Note that the LCCs associated with farmland and urban pixels were excluded from the calculation of the *EDI*. These pixels accounted for a relatively small percentage of the study area and were mainly controlled by anthropogenic factors. Therefore, in this study, the *EDI* was designed to capture the evolution of natural LCCs and was calculated using Equation (3):

$$EDI = \frac{\sum[A_k \times (D_a - D_b)]}{\sum A} \times 100\% \quad (3)$$

where D_a and D_b are the ecological levels in year a and b, respectively, in land-cover transitions associated with land-cover category k (k = 1, 2, …, n); A_k is the area of the land-cover transitions 'from' or 'to' land-cover category k; and $\sum A$ is the statistical area.

Given that each land cover category has an ecological level (Table 1), each land-cover transition would contribute to the upward or downward change in the regional *EDI* value. The regional *EDI* value considers all land-cover transitions and, consequently, indicates the direction in which local ecosystems evolve. A positive regional *EDI* value indicates that the local ecosystem is improving because of the land-cover transitions; a negative regional *EDI* value indicates that the local ecosystem is deteriorating because of the land-cover transitions.

- Artificial change percentage (*ACP*)

The *ACP* evaluates the proportion of the LCCs that is directly linked with human activities. Given that farmland and urban land are two land-cover categories mainly governed by human societies, the *ACP* was used to determine the proportion of dryland changes caused by farming and urbanization. The *ACP* value indicates the extent of human influences on local drylands and was calculated using Equation (4):

$$ACP = \frac{\sum \Delta A_{qk}}{\sum \Delta A_{ij}} \times 100\% \quad (4)$$

where ΔA_{ij} is the absolute area of transitions between category i and category j; $\sum \Delta A_{ij}$ is the total changed area in the statistical area; ΔA_{qk} is the absolute area of transitions between category q and k; and $\sum \Delta A_{qk}$ is the total changed area caused by modifications of artificial land-cover categories (i.e., farmland and urban land). Note that, i, j, and q refer to different land-cover categories, and k refers to artificial land-cover categories. In addition, j is a non-i land-cover category and q is a non-k land-cover category.

3. Results

3.1. Evolution of Global Drylands from 1992 to 2020

3.1.1. Dryland Changes at the Global Scale

At the global scale, complex land-cover transitions occurred during the past 30 years (Tables S3–S5). Overall, the global drylands changed at a certain rate with *RCI* reaching 5.08%. Most land-cover categories remained relatively stable, with the absolute value of *CR* less than 10% (Table 2). The evolutionary direction of global arid ecosystems was encouraging, with a positive *EDI* value of 0.36%. About one-fifth of LCCs in global drylands from 1992 to 2020 were linked with anthropogenic disturbances, as indicated by the *ACP* value of 19.87%. However, it is worth noting that urban land had the highest positive *CR*

(228.18%), and wetland had the lowest negative *CR* (−7.47%). The *CR* values for farmland and grassland increased, whereas those for bare land and shrubland decreased.

Table 2. Rate of change in land cover (*CR*) for eight land-cover categories in four periods (1992–2020, 1992–2000, 2001–2010, and 2011–2020).

Land Covers	*CR* (%)			
	1992–2020	1992–2000	2001–2010	2011–2020
Farmland	3.87	1.97	1.37	0.25
Forest	1.61	−2.03	0.36	4.12
Grassland	3.01	0.02	1.06	1.69
Shrub	−1.55	−0.44	−0.37	−0.71
Wetland	−7.47	−3.23	−4.55	0.60
Urban area	228.18	24.94	56.70	48.88
Bare	−2.09	−0.03	−0.83	−1.12
Others	0.48	−0.30	0.47	0.16

3.1.2. Changes in *RCI*, *CR*, *EDI*, and *ACP* at Continental and Country Scales

Relatively high *RCI* values were observed in Oceania and Asia (Figure 2a). Most countries within these two continents experienced dramatic dryland changes, with *RCI* values exceeding 4%, and thus were the main contributors to the global *RCI* during the past three decades. Although arid ecosystems comprise a large area of North America, the dryland changes showed a relatively low *RCI* value. African countries showed diverse changes in drylands land cover with regard to the *RCI* values.

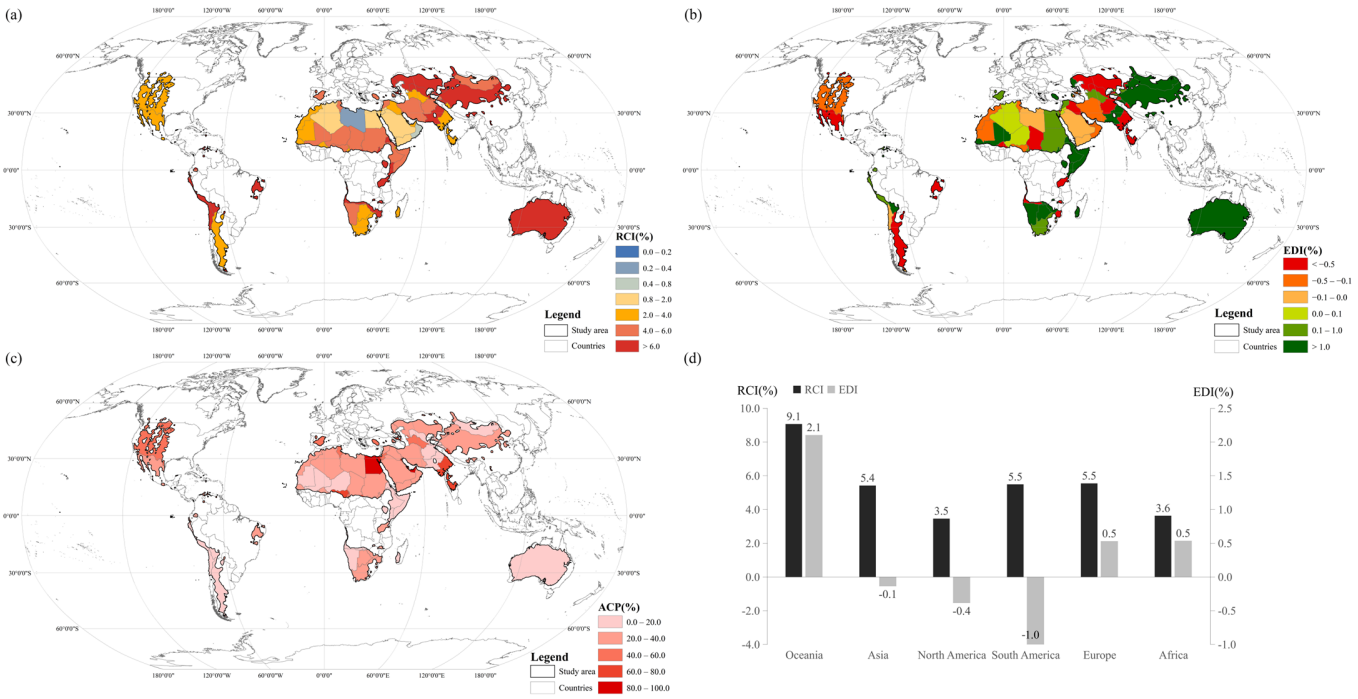

Figure 2. Global dryland change (1992–2020) as indicated by (**a**) regional change intensity (*RCI*), (**b**) evolutionary direction index (*EDI*), (**c**) artificial change percentage (*ACP*), and (**d**) *RCI* and *EDI* at the continental scale.

Seven Asian countries, six African countries, six South American countries, and Australia comprised the 20 top-ranked countries with the highest *RCI* values (Figure 3).

Note that most are developing countries with large dryland areas within their territory. It is, therefore, understandable that complex and intense LCCs occurred in these areas during the past three decades. Specifically, the six African countries, i.e., South Sudan, Kenya, Mozambique, Angola, Zambia, and Zimbabwe, are all located in southeastern Africa. In Asia, the highest *RCI* value was observed in the Central Asia area. Accordingly, southeastern Africa and Central Asia were the most eye-catching regions. The drylands area in South America is small (0.06%), but six of the eight countries with drylands were ranked among the top 20 countries based on *RCI* value.

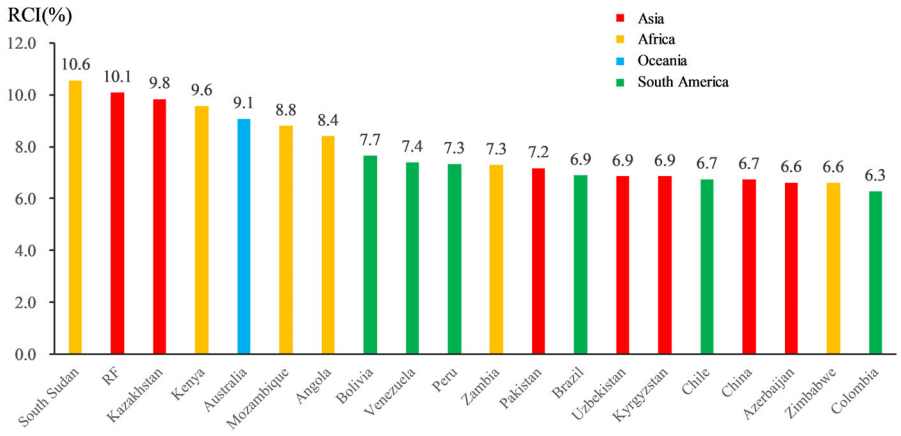

Figure 3. Top 20 countries as ranked by regional change intensity (*RCI*) values.

At the global level, the *CR* values for farmland, forest, and urban land increased, whereas those for bare land decreased. In Asia, Africa, and Oceania, the continental pattern of change in *CR* values was identical to that at the global scale (Table S6). Specifically, Asia accounted for more than 50% of the global increase in urban land. At the same time, Asia lost 21.7 $\times$ 10^4 km^2 of bare land, which was almost half of the global decrease in bare land. Africa experienced a large increase in farmland area and a marked decrease in bare land area, whereas Oceania experienced a large increase in grassland area (12.8 $\times$ 10^4 km^2) and the smallest increase in urban land area. South America lost the largest area of forest compared with all other continents.

The highest positive *EDI* values were observed in Oceania (i.e., Australia) and the Mongolian plateau (i.e., China and Mongolia) (Figure 2b). Several countries in eastern and southern Africa also had positive *EDI* values. Thus, the arid ecosystems in these regions were in better condition in 2020 than in 1992. On the American continents, the arid ecosystems were in worse condition after 29 years. The 10 countries with the highest positive *EDI* values were mainly located in southeastern Africa and Central Asia (Figure 4a). The positive *EDI* values in these two areas and in Australia largely contributed to the global positive *EDI* (0.36%). Note that southeastern Africa and Central Asia were the most eye-catching areas with respect to *RCI* (Figure 3). This indicated that, although these regions experienced intense LCCs during the past three decades, the condition of the arid ecosystems was improved. The *EDI* in Pakistan was 4.9%, and the highest contribution was from the 'bare land to grassland' transition, which accounted for 59.0% of the overall LCC in the country. Certain countries had negative *EDI* values (Figure 4b). For instance, arid ecosystems in Uzbekistan had experienced severe deterioration, with the *EDI* reaching −18.3%. During the past three decades, most pair-year EDIs were negative, which indicated that the deterioration had occurred in most years. More than half (55.9%) of the LCCs were 'wetland (including water bodies) to bare land', which indicated that wetland shrinkage might be the most pressing issue in Uzbekistan.

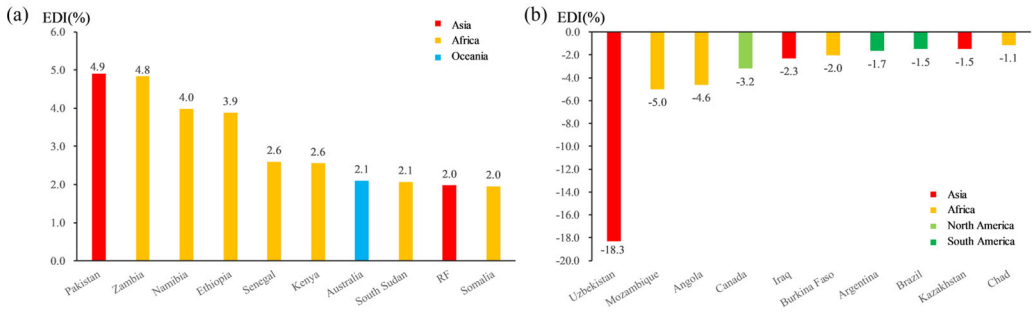

Figure 4. Top 10 countries with the highest positive evolutionary direction index (*EDI*) values (**a**) and top 10 countries with the lowest negative *EDI* values (**b**). Note, 'RF' refers to the Russian Federation.

The *ACP* values in most Asian and African countries remained above 20% (Figure 2c), indicating there were considerable changes to farmland and urban land among arid ecosystems. In contrast, the *ACP* in Oceania was less than 20%. The highest *RCI* and *EDI* values, as well as the lowest *ACP* value, were indicative of the improvement of the natural environment in Oceania. The 10 countries with the highest *ACP* values had notable proportions of drylands changing to urban land and farmland (Figure 5). However, the *EDI* values of these countries were diverse. Three Asian countries, i.e., United Arab Emirates, Azerbaijan, and India, experienced arid ecosystem deterioration and large areas of urbanization and farming activity. This indicated that human activities negatively affected the dryland environment by severely affecting artificial and natural land covers. A similar pattern was observed in the United States. Other countries, for instance, Egypt and Spain, experienced substantial areas of changes in artificial land covers, but the arid ecosystems generally improved.

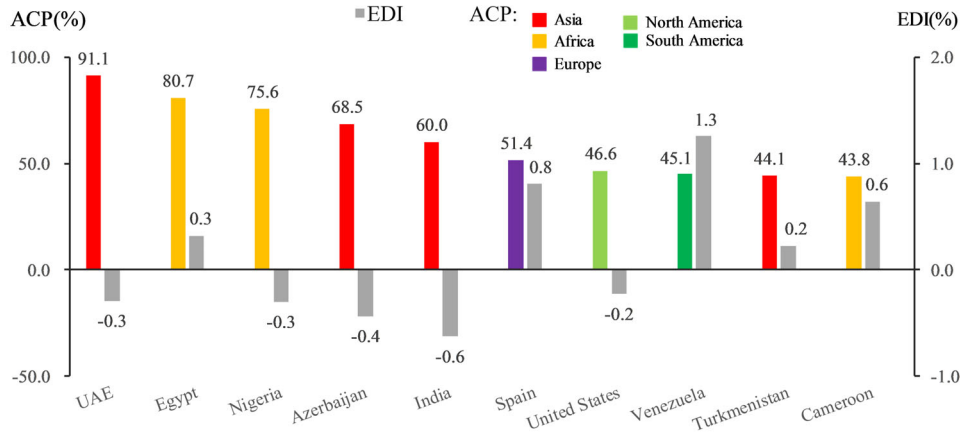

Figure 5. Top 10 countries with the highest artificial change percentage (*ACP*) values. Note, UAE refers to the United Arab Emirates.

The arid ecosystems in Oceania, Europe, and Africa had high *RCI* and positive *EDI* values (Figure 2d). The arid ecosystems in South America and Asia had negative *EDI* and high *RCI* values. South America had the lowest *EDI* (−1.0%), but the *ACP* values in all South American countries remained low. This indicated that the deteriorated arid ecosystems in this continent were the result of indirect human-induced or natural-induced LCCs. Although the *EDI* value in Asia was negative, China had high *RCI* and *EDI* values. However, the *ACP* in China was relatively higher than that observed for other Asian countries (Figure 2c). This indicated that, although farming and urbanization of Chinese drylands had undergone dramatic changes, the natural arid environments were improved during the past 29 years.

3.2. Pair-Year Changes in Global Drylands

3.2.1. Pair-Year *RCI*

Although the global *RCI* (1992–2020) was 5.08%, the *RCI* values in the 28 pair-years were relatively small with values generally less than 0.6% (Figure 6a). This finding is reasonable because LCCs might occur year by year and lead to accumulated consequences over a long period. The pair-year *RCI* went through three phases from 1992 to 2020 (Figure 6a): an increasing trend from 1992 to 1998, a decreasing trend from 1998 to 2014, and another increasing trend after 2014. Overall, the pair-year 2017–2018 had the highest intensity in LCC with the highest *RCI* value of 0.51% compared with all other pair-years.

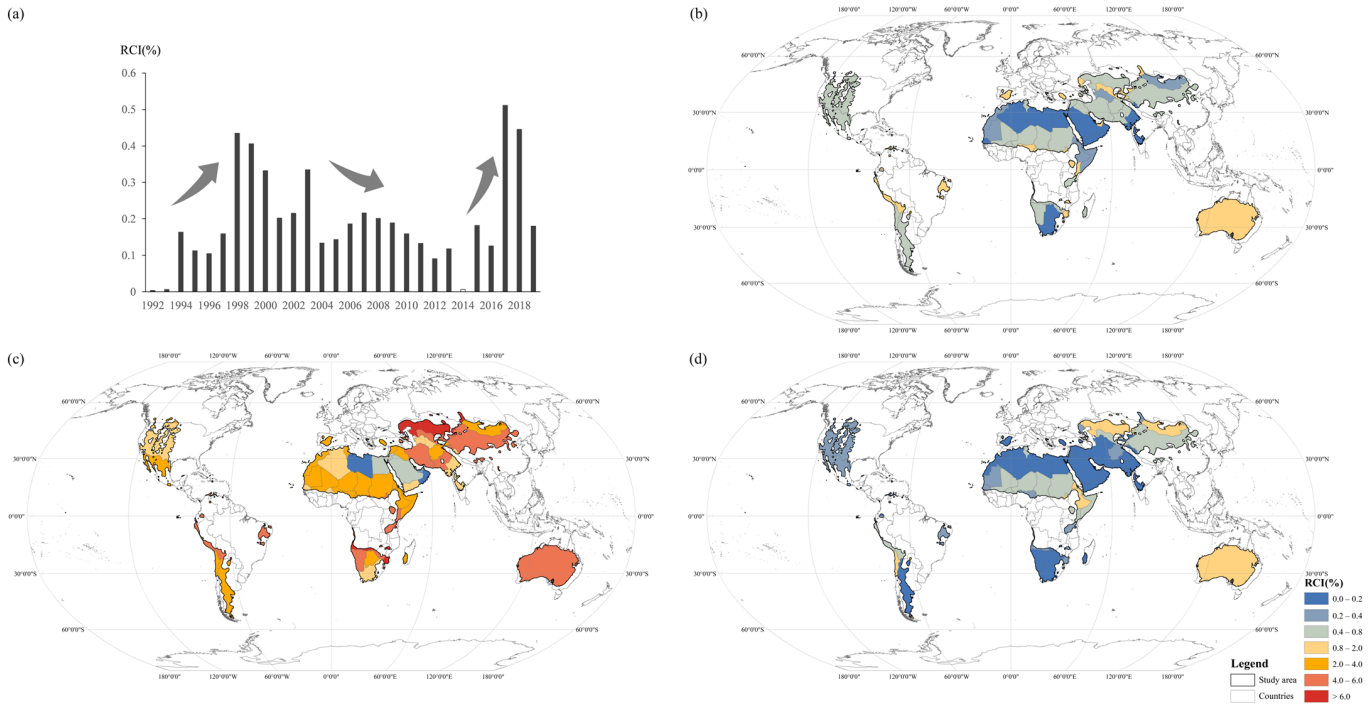

Figure 6. Global regional change intensity (*RCI*) from 1992 to 2020. (**a**) *RCI* values in 28 consecutive pair-years; (**b**) 1992–1998; (**c**) *RCI* (1998–2014); (**d**) *RCI* (2017–2018). The *RCI* value of the pair-year 2014–2015 is marked by a hollow bar.

We calculated the *RCI* values of global drylands in the pair-years 1992–1998 and 1998–2014. The former was 0.55% and the latter was 3.39%. Most countries had larger LCCs in the latter period than in the former period (Figure 6b,c). This finding was in conflict with the observed trends of *RCI* values in these two phases (Figure 6a). However, the increasingly intense dryland dynamics from 1992 to 1998 may occur within approximately the same spatial extent, whereas decreasingly intense dryland dynamics from 1998 to 2014 might have gradually spread to different territories. In addition, the value and spatial distribution of *RCI*s from 2017 to 2018 (Figure 6d) were similar to that derived from the seven-year period (1992–1998) (Figure 6b), which indicated that the global dryland dynamics became increasingly intense and widespread. Countries in northern Africa had consistently low *RCI* values, whereas Australia always had high *RCI* values (Figures 1a and 5b,c). Most countries, especially the Russian Federation and China, showed stronger *RCI* values in the latest 20 years compared with values in the first 10 years.

3.2.2. Pair-Year EDI

As described in Section 3.1.1, the *EDI* (1992–2020) of global arid ecosystems was positive (0.36%). However, the pair-year *EDI* was consistently negative before the pair-year 2002–2003 (Figure 7a). After 2003, the *EDI* was positive in most pair-years and the maximum value was attained in the pair-year 2017–2018. This indicated that the improvements in

global arid ecosystems during the past three decades were mainly because of improvements after 2003. The highest *EDI* in pair-year 2017–2018 was mainly be cause of the LCCs in Australia, Mongolia, Ethiopia, and Somalia (Figure 7d).

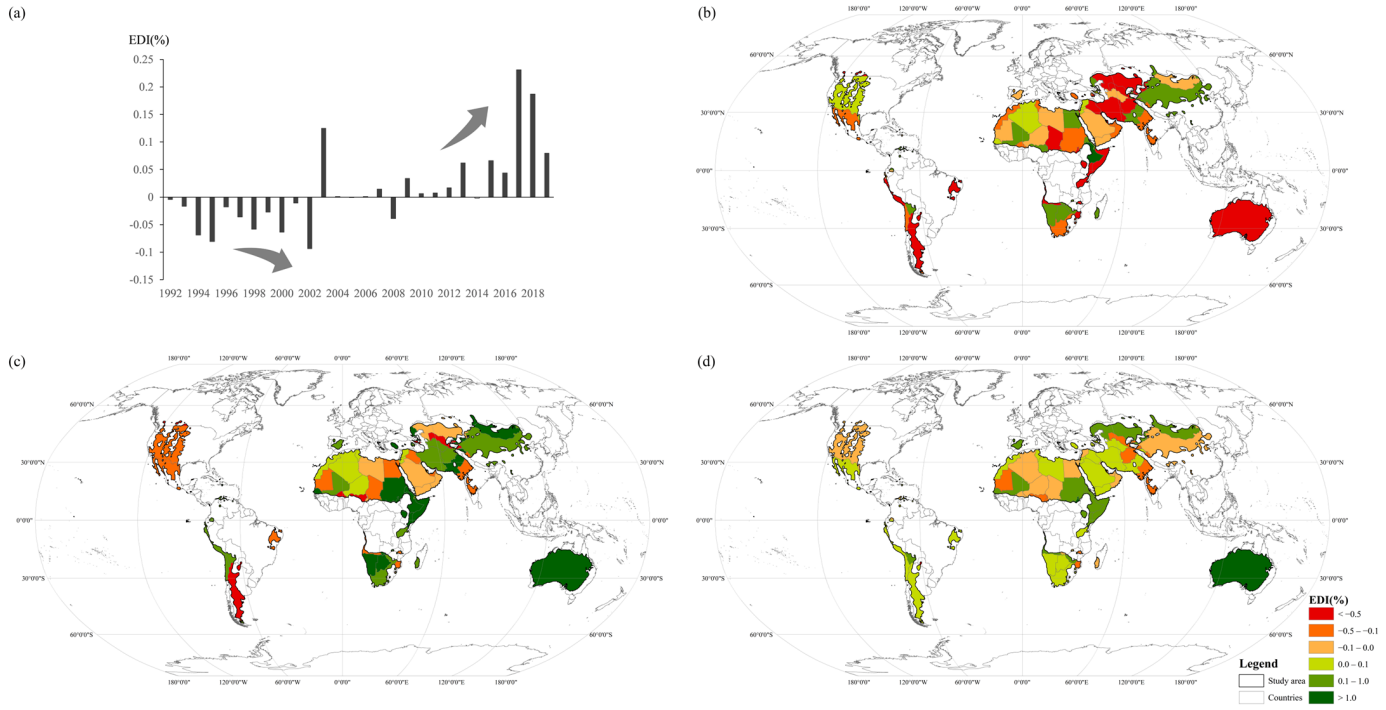

Figure 7. Global evolutionary direction index (*EDI*) from 1992 to 2020. (**a**) *EDI* values in 28 consecutive pair-years; (**b**) 1992–2002; (**c**) 2002–2020; (**d**) 2017–2018. The *EDI* of the pair-year 2014–2015 is marked by a hollow bar.

The *EDI* of global drylands experienced two phases during the past three decades. We further calculated the *EDI* in the pair-years 1992–2002 and 2002–2020. The former value was −0.39% and the latter was 0.74%. Several countries, for instance, Australia, Mongolia, Iran, Somalia, and South Africa, experienced conversion of EDIs from negative to positive (Figure 7b,c), which was consistent with the overall trend in global drylands. The United States experienced a deterioration of *EDI*, which was the opposite of the global overall trend. The *EDI* values remained stable in some countries, such as Libya (consistently negative *EDI*) and China (consistently positive *EDI*). Overall, the improvement of global arid ecosystems during the past three decades was mainly contributed by improvements in Australia, Mongolia, Somalia, and South Africa after 2003. The consistent improvement of arid ecosystems in China also contributed to the overall improvement of global drylands as indicated by the *EDI*.

3.2.3. Pair-Year ACP

The *ACP* values in the 28 consecutive pair-years showed a decreasing trend if the abnormal peak observed in 2014 is excluded (Figure 8a). It is worth noting that the *ACP* declined rapidly during the initial years. After 1995, the *ACP* value fluctuated to a limited extent around 20%. This indicated that the global dryland changes were increasingly contributed by modifications of the natural land-cover categories over time.

The areas of change in continents are shown in Figure 8b. Overall, Asia and Africa experienced the two largest areas of dryland changes. These results were reasonable because most countries in these two continents were agriculture-dominated regions and had experienced rapid urbanization during the past 29 years. In Europe and North America, the areas of change were small, but more than half of these changes were associated with artificial land covers. In South America, more dryland changes occurred, but fewer changes

were caused by artificial land-cover changes, compared with those in Europe and North America. Oceania experienced large areas of dryland changes, but less than 5% of the changes were associated with farming and urbanization.

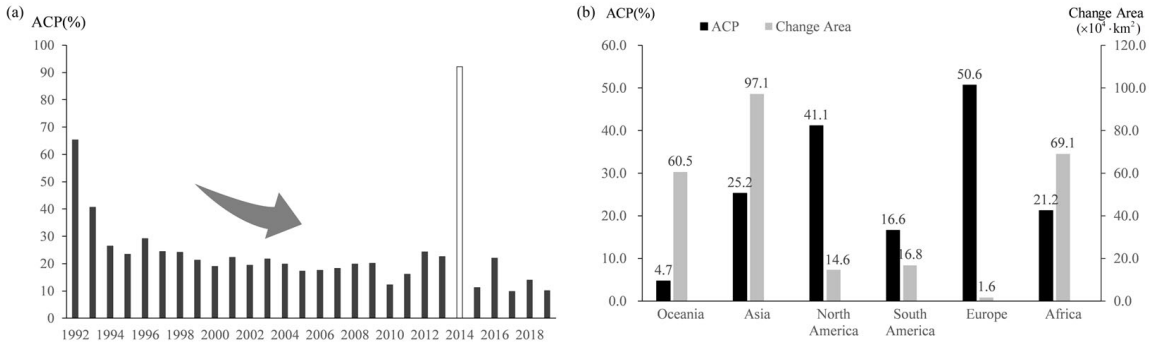

Figure 8. Global artificial change percentage (*ACP*) from 1992 to 2020. (**a**) *ACP* values in the 28 consecutive pair-years; (**b**) *ACP* values and the total areas of change in continents from 1992 to 2020. The *ACP* of the pair-year 2014–2015 is marked by a hollow bar.

4. Discussion

The present study is the first to focus on the evolutionary behavior of global arid ecosystems during the last three decades. In general, the Earth's arid ecosystems evolved with a promising direction from the perspective of LCCs. This conclusion is consistent with previous research using a time-series normalized difference vegetation index [39–41]. However, worldwide drylands experienced different LCCs [62,63] because of differences in human–nature interactions [21,64,65]. It is of considerable interest to understand the diversity and uniqueness, as well as the nonlinear evolutionary paths, of Earth's arid ecosystems.

4.1. Diversity and Uniqueness of Evolution in Global Drylands

The arid ecosystems in Oceania, Central Asia, and southeastern Africa generally improved, despite the intense LCCs in these areas. A previous local study [44] also indicated that Central Asia experienced an overall decrease in bare land and an overall increase in natural land covers from 2001 to 2017; the potential driving factors might be the amount of rainfall and severity of drought [44]. The intensive LCCs in the areas of interest in southeastern Africa were observed from the 1980s to 2013 [47]. The present results further confirmed that the arid ecosystems generally improved. Among hotspot countries, the greening trend in southeastern Australia from 1981 to 2007 has been recorded previously [46,66]. Evidence from previous research supported the finding of a decrease in bare land in Pakistan [13]. The greening of China in recent decades was observed in previous research analyzing a satellite imagery time-series [67]. Many Chinese region-wide eco-projects have been conducted in arid areas [68], which might be the main reason for positive *EDI* and relatively high *RCI* for China. The arid ecosystem has degraded in Uzbekistan because of wetland (including water bodies) shrinkage, which has been recorded in previous studies documenting wetland deterioration in the Amu Darya River Basin and the Aral Sea. The former might be caused by the expansion of farming, reservoirs, and irrigation [49], and the latter is claimed to be driven by global warming and the absence of water-saving technology in farming [69]. The arid ecosystems in South America deteriorated because of intensive natural land-cover transitions. A previous study has reported severe land degradation in Argentina [48].

The uniqueness of evolution in global drylands is shown by the differences with evolution in global non-drylands. First, the decrease in bare land and wetland, as well as the increase in forest and grassland, are distinct with regard to natural LCCs. Bare land accounts for the largest proportion of global drylands and decreased by 43.8×10^4 km^2 with *CR* of −2.09%. Previous evidence also supports the decrease in bare land. However, the extent of the decrease ranged from 75.2×10^4 km^2 [37] to 16.5×10^4 km^2 [35] during

1982–2016, and approximately 50 × 10^4 km^2 during 1992–2018 [36]. Taking into account the most severe decrease (75.2 × 10^4 km^2) recorded in previous research [37], 58.2% of the decrease was in drylands according to the present results. This indicates that the decline in bare land is more serious in drylands than in non-drylands. The wetland (including water bodies and water-covered shrubs/herbaceous) in global drylands decreased with *CR* as high as −7.47%, whereas global evidence indicates an overall increase in permanent surface water area from 1984 to 2015 [51,52]. Although global water monitoring still has numerous challenges [70,71], a previous study on global endorheic basin water [72], which covered approximately the same spatial extent as that observed in the present study, showed a clear trend for decline in water storage (1984–2015). Furthermore, the global forest/tree canopy cover showed a net loss from 1992 to 2018 [36], but the present results showed that forest in drylands experienced a slight increase with *CR* of 1.61%. The grassland/short vegetation cover showed a net loss [35,37], but in the present study, grassland slightly increased in global drylands with *CR* of 3.01%. The global loss of forest and grassland has mainly occurred in non-drylands. The greening in natural land cover generally portrays a unique and encouraging evolution in global drylands. These findings explain the overall positive *EDI* and may be associated with recent evidence of climate change in drylands [4,44].

Although we observed an overall promising evolution in global drylands during the past 30 years, an opposing trend is the rapid expansion of urban land and farming. Urbanization in drylands is more rapid than that in global non-drylands. The *CR* of urban land reached 228.2% in drylands (Table S4), whereas a global *CR* of 126.1% was reported in previous research [39]. Although the extents of increase in urbanization in previous studies differed because of disparity in the definitions of urban and dryland areas [14,36], there is no doubt that rapid urban expansion in drylands is a worldwide phenomenon. Globally, farmland increased by 100 × 10^4 km^2 during 1992–2018 [36], but farmland in drylands only increased by 22.3 × 10^4 km^2 from 1992 to 2020. This indicates that the worldwide increase in farmland has mainly occurred in non-drylands. Given that anthropogenic consequences are usually permanent, the dramatically increasing artificial land covers indicate that cautious steps are required to avoid potential issues caused by rapid urbanization and for long-term sustainable development in global drylands.

4.2. Nonlinear Evolutionary Paths of Global Arid Ecosystems

The nonlinear evolutionary paths of global arid ecosystems are difficult to discern from previous LCC studies. Traditionally, LCC information is obtained based on the existing land-cover maps, i.e., the so-called 'post-classification' change detection strategy [59]. Previous LCC studies using this strategy usually summarized LCCs by comparing land-cover information in selected and limited years [35,37,39]. The evolutionary processes determined by these studies might be approximate, and even biased, because the results were mainly shaped and restrained by the preliminary selected temporal phases. In contrast, in the present study, a long-term LCC dataset (1992–2020), combined with detailed changes occurring in 28 consecutive pair-years, jointly portrayed the nonlinear evolutionary pathway for global drylands in the past three decades.

Although the present results (for the period 1992–2020) proved that global drylands seemed stable and global arid ecosystems even improved slightly in recent decades, the optimistic situation was not achieved through a linear process. Tortuous paths were reflected in long-term *RCI*, *EDI*, and *ACP* values. With respect to *RCI*, differences in the extents of *RCI* were differentiable into three phases, namely, 'intense' during 1992–1998, 'stable' during 1998–2014, and 'intense' during 2014–2020. Considering EDI, the evolution of global arid ecosystems went through two periods, i.e., remaining consistently deteriorating before 2003 and assuming a promising direction after 2003. These nonlinear changes are closely associated with the nonlinear changes in climatic factors or human activities. Previous studies have reported that the climate [28,73,74], human impacts on the Earth's systems [75,76], and even the relationship between vegetation greenness and rainfall [77] have all experienced frequently nonlinear changes in the past. However, because of

the differences in study areas, study periods, research objects (satellite-based vegetation indicators, thematic LCC, or comprehensive indicators derived from general LCCs), and the method of nonlinear diagnosis (statistical analysis of vegetation trajectories or observation of annual consequence of general LCCs), the derived results are not comparable. We believed these results are not conflicting, but rather represent different perspectives of the Earth's evolution and may be supplementary to obtain rich background information on global dryland evolution.

With regard to ACPs, the current results indicated a consistent decline in the contributions from urbanization and farming to the global dryland changes (excluding 2014). However, it may not necessarily imply that anthropogenic interferences for global drylands have decreased. Based on the existing evidence [78–80], a more likely explanation is that society is changing the methods of exploiting arid ecosystems. Humans might instead turn to modification of other land covers or influence drylands through indirect measures.

4.3. Limitation and Outlook

The present study used the most recent version of the global climate map using the Köppen–Geiger system (released in 2020) to determine the geographical extent of global drylands. Therefore, the evaluations in this study are only relevant within this area, assuming that the area of global drylands is stable. However, previous research has proven that the extent of global drylands has changed in recent years [4,33,62]. Future studies could capture LCC characteristics in dynamic scenarios by updating the extent of drylands.

The present analyses were based on the CCILC dataset because of its advantages in long-term data accumulation and broad application at the global scale [20,36,55]. However, the present findings will contain a certain level of uncertainty related to the following aspects of the CCILC dataset. First, the coarse spatial resolution (300 m) of the CCILC dataset would instinctively lead to mixed pixels, which would influence the calculated area of land covers and their corresponding changes [20]. Further studies using datasets with relatively higher spatial resolution are required. Second, the accuracy of the CCILC dataset, including an overall accuracy of approximately 71.45%, different accuracies of land-cover categories, and the temporal inconsistency, would cause error accumulation and propagation effects, leading to spurious changes to some extent. Previous studies have shown that the product of individual map accuracies determines the accuracy of LCCs [22,81]. In particular, the temporal consistency of the CCILC dataset has received considerable attention because the data are based on imagery from multiple satellite sources [82]. The producers used a 'baseline' and a uniform legend to ensure consistency between the map series. Although previous studies assessed its temporal consistency [83] and compared the CCILC dataset with other land-cover products [20,55], these studies only targeted limited countries or areas of interest. To date, the global performance of its temporal consistency remains uncertain. In the present work, a noteworthy phenomenon is that the *RCI*, *EDI*, and *ACP* in 2014 were 0.0066, −0.0021, and 92.1%, respectively. This indicates that, during 2014 and 2015, the total change areas of global drylands remained extremely small, but 92.1% of the changes were associated with urbanization and farming. More importantly, the arid ecosystems deteriorated slightly because of these changes. These abnormal results indicate that the land-cover map for 2014 might be extremely similar to that of 2015, especially in the distributions of natural land covers. Given that the official documentation acknowledged that the changes occurring during 2014–2015 are limited to certain changes [84], users are warned to be cautious of the LCC information during 2014–2015. It is impossible to validate an individual global map of the CCILC dataset, and hence it is difficult to assess the influences of these uncertainties on the present results. Further studies could build on the present results by developing high-quality time-series LCC products.

The EDI, which was conceived using information on LCCs, was used to indicate the direction of evolution in arid ecosystems. However, multiple indicators could be used to estimate eco-evolution from different perspectives. Further studies on the use

of various indicators to estimate eco-evolution are warranted. The present study sheds light on the drivers of LCCs in arid ecosystems by targeting urbanization and farming activities. However, numerous external interferences would influence the processes of LCC in drylands during the last three decades. For instance, variation in precipitation and temperature may cause the shrinkage or expansion of wetlands. Various human activities, such as afforestation, grazing prohibition, and rest–rotation grazing, may have shaped the LCCs in global drylands. Further research is recommended on the use of indicators involving multiple drivers to obtain further information on the processes responsible.

5. Conclusions

Analysis of LCCs in global drylands is important for understanding the evolutionary mechanisms of global arid ecosystems. This study is the first to explore long-term dryland dynamics at the global scale. Four indicators, i.e., *RCI*, *CR*, *EDI*, and *ACP*, were used to capture the intensity, rate, evolutionary direction, and potential drivers of global dryland change. We examined the characteristics of LCC at the global, continental, and country scales, and several hotspots with eye-catching LCCs were highlighted. From a temporal perspective, the long-term changes (1992–2020) and the annual changes in 28 consecutive pair-years were targeted to represent the nonlinear evolutionary path of global arid ecosystems. In this manner, the pathway, direction, and anthropogenic interferences of the evolution of global arid ecosystems were examined. The main findings and inferences were as follows:

(1) From 1992 to 2020, the global *RCI*, *EDI*, and *ACP* were 5.08, 0.36, and 19.87%, respectively. This indicated that global arid ecosystems generally evolved in a promising direction despite certain LCCs and human interferences. However, cautious steps are required to avoid potential issues caused by rapid urbanization and farming expansion in global drylands.

(2) Several hotspot drylands were observed. The arid ecosystems in Australia were improved, but the lowest *ACP* indicated that the improvements were mainly associated with natural factors. Although arid ecosystems in Asia deteriorated, as indicated by the negative *EDI*, many Asian countries were noteworthy. The arid environments in China improved despite intensive LCCs and dramatic urbanization and farming expansion; the arid environments in Pakistan improved mainly because of large areas changing from bare land to grassland. The arid environments in southeastern Africa generally improved with intensive LCCs during the past three decades. The arid ecosystems in North American countries deteriorated, with 41.1% of changes caused by urbanization or farming. The arid ecosystems in South American countries also deteriorated, but 83.4% of changes were associated with changes in natural land covers. The arid ecosystems in Europe generally improved, although 50.6% of the changes were associated with urbanization and farming activities.

(3) Global arid ecosystems experienced three phases, as indicated by *RCI* values: intensive change with increase in *RCI* values (1992–1998); stable with decline in *RCI* values (1998–2014); and intensive change with increase in *RCI* values (2015–2020). Two phases were differentiated based on *EDI* values, namely, a 'deterioration' period with mainly negative *EDI* values (1992–2002), and an 'improvement' period with mainly positive *EDI* values after 2002. The *ACP* values, in general, decreased over time, providing a clear indication that urbanization and farming gradually contributed less to dryland change (excluding 2014).

The highlighted hotspots provide evidence for the diversity of evolution in global drylands. The results inferred that urban land increased more rapidly in drylands than in non-drylands, but that farmland in drylands expanded more slowly than in non-drylands. The overall global decrease in bare land mainly occurred in drylands. Forest and grassland increased in drylands but decreased at a global scale. In contrast, wetland decreased in drylands but increased globally. These findings demonstrated the uniqueness of evolution in global drylands. The nonlinear evolutionary pathway for global dryland dynamics in the

past three decades provides insights into the evolutionary mechanism for arid ecosystems worldwide. Further research is required using dynamic scenarios for drylands, remote sensing products with higher overall accuracy and improved temporal consistency, and multiple statistical indicators to build on the present results.

Supplementary Materials: The following supporting information can be downloaded at: https://www.mdpi.com/article/10.3390/rs15123178/s1, Figure S1: The study area; Table S1: The study area and the covering countries around continents; Table S2: The 37 land cover categories in CCILI dataset and their re-groups; Table S3: The transition matrix (%) of eight land cover categories (1992–2020); Table S4: The CRs in 37 land cover categories (1992–2020); Table S5: Top eight land cover transitions from 1992 to 2020(%); Table S6: Net change areas ($\times 10^4$ km^2) of 8 land cover categories in continents.

Author Contributions: Conceptualization, L.X., B.L. and N.-E.T.; data curation, L.X. and T.C.; formal analysis, L.X., B.L. and N.-E.T.; funding acquisition, L.X.; investigation, L.X., B.L. and N.-E.T.; methodology, L.X., T.C., B.L., Y.Y. and N.-E.T.; project administration: L.X.; software, Y.Y., L.X. and T.C.; validation, L.X. and T.C.; visualization, L.X. and T.C.; writing original draft preparation, L.X.; writing review and editing, L.X., B.L. and N.-E.T. All authors have read and agreed to the published version of the manuscript.

Funding: This study was funded by the National Natural Science Foundation of China (grant no. 41701474), the National Key Research and Development Plan of China (grant no. 2016YFC0500205), and the National Basic Research Program of China (grant no. 2015CB954103).

Data Availability Statement: The CCILC dataset comes from the official website of the European Space Agency (https://www.esa-landcover-cci.org (accessed on 25 June 2022)), and the global climate map comes from the Global Groundwater Information System website (https://ggis.un-igrac.org/catalogue/#/dataset/431 (accessed on 4 May 2023)).

Acknowledgments: The authors are deeply grateful to Dengsheng Lu for his thoughtful reviews and constructive comments. The authors are grateful to the editor and anonymous reviewers whose comments have contributed to improving the quality of the paper.

Conflicts of Interest: The authors declare no conflict of interest.

References

1. Ahlström, A.; Raupach, M.R.; Schurgers, G.; Smith, B.; Arneth, A.; Jung, M.; Reichstein, M.; Canadell, J.G.; Friedlingstein, P.; Jain, A.K.; et al. The dominant role of semi-arid ecosystems in the trend and variability of the land CO_2 sink. *Science* **2015**, *348*, 895–899. [CrossRef] [PubMed]
2. Fu, B.; Stafford-Smith, M.; Wang, Y.; Wu, B.; Yu, X.; Lv, N.; Ojima, D.S.; Lv, Y.; Fu, C.; Liu, Y.; et al. The Global-DEP conceptual framework—Research on dryland ecosystems to promote sustainability. *Curr. Opin. Environ. Sustain.* **2020**, *48*, 17–28. [CrossRef]
3. Aranibar, J.N.; Anderson, I.; Ringrose, S.; Macko, S.J. Importance of nitrogen fixation in soil crusts of southern African arid ecosystems: Acetylene reduction and stable isotope studies. *J. Arid. Environ.* **2003**, *54*, 345–358. [CrossRef]
4. Huang, J.; Fu, C.; Chen, F.; Fu, Q.; Dai, A.; Shinoda, M.; Ma, Z.; Guo, W.; Li, Z.; Zhang, L.; et al. Dryland climate change: Recent progress and challenges. *Rev. Geophys.* **2017**, *55*, 719–778. [CrossRef]
5. Poulter, B.; Frank, D.; Ciais, P.; Myneni, R.B.; Andela, N.; Bi, J.; Broquet, G.; Canadell, J.G.; Chevallier, F.; Liu, Y.Y.; et al. Contribution of semi-arid ecosystems to interannual variability of the global carbon cycle. *Nature* **2014**, *509*, 600–603. [CrossRef]
6. Xu, L.; Yu, G.; Zhang, W.; Tu, Z.; Tan, W. Change features of time-series climate variables from 1962 to 2016 in Inner Mongolia, China. *J. Arid. Land* **2020**, *12*, 58–72. [CrossRef]
7. Chen, B.; Zhang, X.; Tao, J.; Wu, J.; Wang, J.; Shi, P.; Zhang, Y.-J.; Yu, C. The impact of climate change and anthropogenic activities on alpine grassland over the Qinghai-Tibet Plateau. *Agric. For. Meteorol.* **2014**, *189*, 11–18. [CrossRef]
8. Guirado, E.; Delgado-Baquerizo, M.; Martínez-Valderrama, J.; Tabik, S.; Alcaraz-Segura, D.; Maestre, F.T. Climate legacies drive the distribution and future restoration potential of dryland forests. *Nat. Plants* **2022**, *8*, 879–886. [CrossRef]
9. Huete, A. ECOLOGY Vegetation's responses to climate variability. *Nature* **2016**, *531*, 181–182. [CrossRef]
10. Flombaum, P.; Yahdjian, L.; Sala, O.E. Global-change drivers of ecosystem functioning modulated by natural variability and saturating responses. *Glob. Chang. Biol.* **2016**, *23*, 503–511. [CrossRef]
11. Schlaepfer, D.R.; Bradford, J.B.; Lauenroth, W.K.; Munson, S.M.; Tietjen, B.; Hall, S.A.; Wilson, S.D.; Duniway, M.C.; Jia, G.; Pyke, D.A.; et al. Climate change reduces extent of temperate drylands and intensifies drought in deep soils. *Nat. Commun.* **2017**, *8*, 14196. [CrossRef] [PubMed]

12. Koutroulis, A.G. Dryland changes under different levels of global warming. *Sci. Total. Environ.* **2019**, *655*, 482–511. [CrossRef] [PubMed]
13. Arshad, S.; Hasan Kazmi, J.; Fatima, M.; Khan, N.J.A.G. Change detection of land cover/land use dynamics in arid region of Bahawalpur District, Pakistan. *Appl. Geomat.* **2022**, *14*, 387–403. [CrossRef]
14. Ren, Q.; He, C.; Huang, Q.; Shi, P.; Da Zhang, D.; Güneralp, B. Impacts of urban expansion on natural habitats in global drylands. *Nat. Sustain.* **2022**, *5*, 869–878. [CrossRef]
15. Wagner, F.H.; Hérault, B.; Rossi, V.; Hilker, T.; Maeda, E.E.; Sanchez, A.; Lyapustin, A.I.; Galvão, L.S.; Wang, Y.; Aragão, L.E.O.C. Climate drivers of the Amazon forest greening. *PLoS ONE* **2017**, *12*, e0180932. [CrossRef]
16. Garcia, R.A.; Cabeza, M.; Rahbek, C.; Araújo, M.B. Multiple Dimensions of Climate Change and Their Implications for Biodiversity. *Science* **2014**, *344*, 1247579. [CrossRef]
17. Halsch, C.A.; Shapiro, A.M.; Fordyce, J.A.; Nice, C.C.; Thorne, J.H.; Waetjen, D.P.; Forister, M.L. Insects and recent climate change. *Proc. Natl. Acad. Sci. USA* **2021**, *118*, e2002543117. [CrossRef]
18. Noyes, P.D.; McElwee, M.; Miller, H.D.; Clark, B.W.; Van Tiem, L.A.; Walcott, K.C.; Erwin, K.N.; Levin, E.D. The toxicology of climate change: Environmental contaminants in a warming world. *Environ. Int.* **2009**, *35*, 971–986. [CrossRef] [PubMed]
19. Huang, J.; Yu, H.; Guan, X.; Wang, G.; Guo, R. Accelerated dryland expansion under climate change. *Nat. Clim. Chang.* **2016**, *6*, 166–171. [CrossRef]
20. Liu, X.; Yu, L.; Li, W.; Peng, D.; Zhong, L.; Li, L.; Xin, Q.; Lu, H.; Yu, C.; Gong, P. Comparison of country-level cropland areas between ESA-CCI land cover maps and FAOSTAT data. *Int. J. Remote Sens.* **2018**, *39*, 6631–6645. [CrossRef]
21. Zhang, L.; Yang, L.; Zohner, C.M.; Crowther, T.W.; Li, M.; Shen, F.; Guo, M.; Qin, J.; Yao, L.; Zhou, C. Direct and indirect impacts of urbanization on vegetation growth across the world's cities. *Sci. Adv.* **2022**, *8*, eabo0095. [CrossRef]
22. Xu, L.; Herold, M.; Tsendbazar, N.-E.; Masiliūnas, D.; Li, L.; Lesiv, M.; Fritz, S.; Verbesselt, J. Time series analysis for global land cover change monitoring: A comparison across sensors. *Remote Sens. Environ.* **2022**, *271*, 112905. [CrossRef]
23. Song, W.; Deng, X. Land-use/land-cover change and ecosystem service provision in China. *Sci. Total. Environ.* **2017**, *576*, 705–719. [CrossRef]
24. Bregman, T.P.; Lees, A.C.; MacGregor, H.E.A.; Darski, B.; de Moura, N.G.; Aleixo, A.; Barlow, J.; Tobias, J.A. Using avian functional traits to assess the impact of land-cover change on ecosystem processes linked to resilience in tropical forests. *Proc. R. Soc. B Boil. Sci.* **2016**, *283*, 20161289. [CrossRef]
25. Santos, M.J.; Smith, A.B.; Dekker, S.C.; Eppinga, M.B.; Leitão, P.J.; Moreno-Mateos, D.; Morueta-Holme, N.; Ruggeri, M. The role of land use and land cover change in climate change vulnerability assessments of biodiversity: A systematic review. *Landsc. Ecol.* **2021**, *36*, 3367–3382. [CrossRef]
26. Reinhart, V.; Hoffmann, P.; Rechid, D.; Böhner, J.; Bechtel, B. High-resolution land use and land cover dataset for regional climate modelling: A plant functional type map for Europe 2015. *Earth Syst. Sci. Data* **2022**, *14*, 1735–1794. [CrossRef]
27. Zhang, J.; Ren, M.; Lu, X.; Li, Y.; Cao, J. Effect of the Belt and Road Initiatives on Trade and Its Related LUCC and Ecosystem Services of Central Asian Nations. *Land* **2022**, *11*, 828. [CrossRef]
28. Xu, L.; Yu, G.; Tu, Z.; Zhang, Y.; Tsendbazar, N.-E. Monitoring vegetation change and their potential drivers in Yangtze River Basin of China from 1982 to 2015. *Environ. Monit. Assess.* **2020**, *192*, 642. [CrossRef] [PubMed]
29. Xu, L.; Li, B.; Yuan, Y.; Gao, X.; Zhang, T.; Sun, Q. Detecting Different Types of Directional Land Cover Changes Using MODIS NDVI Time Series Dataset. *Remote Sens.* **2016**, *8*, 495. [CrossRef]
30. Gómez, C.; White, J.C.; Wulder, M.A. Optical remotely sensed time series data for land cover classification: A review. *ISPRS J. Photogramm. Remote Sens.* **2016**, *116*, 55–72. [CrossRef]
31. Phiri, D.; Simwanda, M.; Salekin, S.; Nyirenda, V.R.; Murayama, Y.; Ranagalage, M. Sentinel-2 Data for Land Cover/Use Mapping: A Review. *Remote Sens.* **2020**, *12*, 2291. [CrossRef]
32. Zhu, Z. Change detection using landsat time series: A review of frequencies, preprocessing, algorithms, and applications. *ISPRS J. Photogramm. Remote Sens.* **2017**, *130*, 370–384. [CrossRef]
33. Li, C.; Fu, B.; Wang, S.; Stringer, L.C.; Wang, Y.; Li, Z.; Liu, Y.; Zhou, W. Drivers and impacts of changes in China's drylands. *Nat. Rev. Earth Environ.* **2021**, *2*, 858–873. [CrossRef]
34. Betru, T.; Tolera, M.; Sahle, K.; Kassa, H. Trends and drivers of land use/land cover change in Western Ethiopia. *Appl. Geogr.* **2019**, *104*, 83–93. [CrossRef]
35. Liu, H.; Gong, P.; Wang, J.; Clinton, N.; Bai, Y.; Liang, S. Annual dynamics of global land cover and its long-term changes from 1982 to 2015. *Earth Syst. Sci. Data* **2020**, *12*, 1217–1243. [CrossRef]
36. Radwan, T.M.; Blackburn, G.A.; Whyatt, J.D.; Atkinson, P.M. Global land cover trajectories and transitions. *Sci. Rep.* **2021**, *11*, 12814. [CrossRef]
37. Song, X.-P.; Hansen, M.C.; Stehman, S.V.; Potapov, P.V.; Tyukavina, A.; Vermote, E.F.; Townshend, J.R. Global land change from 1982 to 2016. *Nature* **2018**, *560*, 639–643. [CrossRef]
38. Li, W.; Ciais, P.; MacBean, N.; Peng, S.; Defourny, P.; Bontemps, S. Major forest changes and land cover transitions based on plant functional types derived from the ESA CCI Land Cover product. *Int. J. Appl. Earth Obs. Geoinf.* **2016**, *47*, 30–39. [CrossRef]
39. He, B.; Wang, S.; Guo, L.; Wu, X. Aridity change and its correlation with greening over drylands. *Agric. For. Meteorol.* **2019**, *278*, 107663. [CrossRef]

40. He, L.; Guo, J.; Yang, W.; Jiang, Q.; Chen, L.; Tang, K. Multifaceted responses of vegetation to average and extreme climate change over global drylands. *Sci. Total Environ.* **2022**, *858 Pt 2*, 159942. [CrossRef]
41. Burrell, A.L.; Evans, J.P.; De Kauwe, M.G. Anthropogenic climate change has driven over 5 million km^2 of drylands towards desertification. *Nat. Commun.* **2020**, *11*, 3853. [CrossRef]
42. Zhang, G.; Biradar, C.M.; Xiao, X.; Dong, J.; Zhou, Y.; Qin, Y.; Zhang, Y.; Liu, F.; Ding, M.; Thomas, R.J. Exacerbated grassland degradation and desertification in Central Asia during 2000–2014. *Ecol. Appl.* **2018**, *28*, 442–456. [CrossRef]
43. Tew, Y.L.; Tan, M.L.; Kwok, P.C.; Samat, N.; Mahamud, M.A. Analysis of the Relationship between Climate Change and Land Use Change using the ESA CCI Land Cover Maps in Sungai Kelantan Basin, Malaysia. *Sains Malays.* **2022**, *51*, 437–449. [CrossRef]
44. Hu, Y.; Hu, Y. Land Cover Changes and Their Driving Mechanisms in Central Asia from 2001 to 2017 Supported by Google Earth Engine. *Remote Sens.* **2019**, *11*, 554. [CrossRef]
45. Chen, C.; Park, T.; Wang, X.; Piao, S.; Xu, B.; Chaturvedi, R.K.; Fuchs, R.; Brovkin, V.; Ciais, P.; Fensholt, R.; et al. China and India lead in greening of the world through land-use management. *Nat. Sustain.* **2019**, *2*, 122–129. [CrossRef] [PubMed]
46. Deng, Y.; Wang, S.; Bai, X.; Luo, G.; Wu, L.; Chen, F.; Wang, J.F.; Li, C.J.; Yang, Y.J.; Hu, Z.Y.; et al. Vegetation greening intensified soil drying in some semi-arid and arid areas of the world. *Agric. For. Meteorol.* **2020**, *292*, 108103. [CrossRef]
47. Bailey, K.M.; McCleery, R.A.; Binford, M.W.; Zweig, C. Land-cover change within and around protected areas in a biodiversity hotspot. *J. Land Use Sci.* **2016**, *11*, 154–176. [CrossRef]
48. Fernández, D.S.; Puchulu, M.E.; Rostagno, M.C.; Manna, L.L.; Becker, A.R.; Grumelli, M.D.; Schiavo, H.F. Agricultural Land Degradation in Argentina. In *The Handbook of Environmental Chemistry*; Springer: Berlin/Heidelberg, Germany, 2022. [CrossRef]
49. Zan, C.; Liu, T.; Huang, Y.; Bao, A.; Yan, Y.; Ling, Y.; Wang, Z.; Duan, Y. Spatial and temporal variation and driving factors of wetland in the Amu Darya River Delta, Central Asia. *Ecol. Indic.* **2022**, *139*, 108898. [CrossRef]
50. Jeong, S.-J.; Ho, C.-H.; Brown, M.E.; Kug, J.-S.; Piao, S. Browning in desert boundaries in Asia in recent decades. *J. Geophys. Res. Atmos.* **2011**, *116*. [CrossRef]
51. Hou, J.; van Dijk, A.I.J.M.; Beck, H.E.; Renzullo, L.J.; Wada, Y. Remotely sensed reservoir water storage dynamics (1984–2015) and the influence of climate variability and management at a global scale. *Hydrol. Earth Syst. Sci.* **2022**, *26*, 3785–3803. [CrossRef]
52. Pekel, J.-F.; Cottam, A.; Gorelick, N.; Belward, A.S. High-resolution mapping of global surface water and its long-term changes. *Nature* **2016**, *540*, 418–422. [CrossRef]
53. He, C.; Liu, Z.; Gou, S.; Zhang, Q.; Zhang, J.; Xu, L. Detecting global urban expansion over the last three decades using a fully convolutional network. *Environ. Res. Lett.* **2019**, *14*, 034008. [CrossRef]
54. Peel, M.C.; Finlayson, B.L.; McMahon, T.A. Updated world map of the Köppen-Geiger climate classification. *Hydrol. Earth Syst. Sci.* **2007**, *11*, 1633–1644. [CrossRef]
55. Wang, L.; Bartlett, P.; Pouliot, D.; Chan, E.; Lamarche, C.; Wulder, M.A.; Defourny, P.; Brady, M. Comparison and Assessment of Regional and Global Land Cover Datasets for Use in CLASS over Canada. *Remote Sens.* **2019**, *11*, 2286. [CrossRef]
56. Li, W.; MacBean, N.; Ciais, P.; Defourny, P.; Lamarche, C.; Bontemps, S.; Houghton, R.A.; Peng, S. Gross and net land cover changes in the main plant functional types derived from the annual ESA CCI land cover maps (1992–2015). *Earth Syst. Sci. Data* **2018**, *10*, 219–234. [CrossRef]
57. Wang, X.F.; Lesi, M.C.; Zhang, M.M. Ecosystem pattern change and its influencing factors of "two barriers and three belts". *Chin. J. Ecol.* **2019**, *38*, 2138–2148. (In Chinese) [CrossRef]
58. Shao, Q.Q.; Liu, J.Y.; Huang, L.; Fan, J.W.; Xu, X.L.; Wang, J.B. Integrated assessment on the effectiveness of ecological conservation in Sanjiangyuan National Nature Reserve. *Geogr. Res.* **2013**, *32*, 1645–1656. (In Chinese) [CrossRef]
59. Colditz, R.R.; Acosta-Velázquez, J.; Gallegos, J.R.D.; Lule, A.D.V.; Rodríguez-Zúñiga, M.T.; Maeda, P.; López, M.I.C.; Ressl, R. Potential effects in multi-resolution post-classification change detection. *Int. J. Remote Sens.* **2012**, *33*, 6426–6445. [CrossRef]
60. Xie, G.D.; Zhen, L.; Lu, C.X.; Xiao, Y.; Chen, C. Expert Knowledge Based Valuation Method of Ecosystem Services in China. *J. Nat. Resour.* **2008**, *23*, 911–919. Available online: http://www.jnr.ac.cn/EN/10.11849/zrzyxb.2008.05.019 (accessed on 25 June 2022). (In Chinese)
61. Stoner, C.; Caro, T.; Mduma, S.; Mlingwa, C.; Sabuni, G.; Borner, M. Assessment of Effectiveness of Protection Strategies in Tanzania Based on a Decade of Survey Data for Large Herbivores. *Conserv. Biol.* **2007**, *21*, 635–646. [CrossRef] [PubMed]
62. Craine, J.M.; Ocheltree, T.W.; Nippert, J.B.; Towne, E.G.; Skibbe, A.M.; Kembel, S.W.; Fargione, J.E. Global diversity of drought tolerance and grassland climate-change resilience. *Nat. Clim. Chang.* **2013**, *3*, 63–67. [CrossRef]
63. van de Koppel, J.; Rietkerk, M. Spatial Interactions and Resilience in Arid Ecosystems. *Am. Nat.* **2004**, *163*, 113–121. [CrossRef] [PubMed]
64. Assal, T.J.; Anderson, P.J.; Sibold, J. Spatial and temporal trends of drought effects in a heterogeneous semi-arid forest ecosystem. *For. Ecol. Manag.* **2016**, *365*, 137–151. [CrossRef]
65. Saatkamp, A.; Römermann, C.; Dutoit, T. Plant Functional Traits Show Non-Linear Response to Grazing. *Folia Geobot.* **2010**, *45*, 239–252. [CrossRef]
66. Fensholt, R.; Langanke, T.; Rasmussen, K.; Reenberg, A.; Prince, S.D.; Tucker, C.; Scholes, R.; Quang, B.; Bondeau, A.; Eastman, R.; et al. Greenness in semi-arid areas across the globe 1981–2007—An Earth Observing Satellite based analysis of trends and drivers. *Remote Sens. Environ.* **2012**, *121*, 144–158. [CrossRef]

67. Chen, T.; Bao, A.; Jiapaer, G.; Guo, H.; Zheng, G.; Jiang, L.; Chang, C.; Tuerhanjiang, L. Disentangling the relative impacts of climate change and human activities on arid and semiarid grasslands in Central Asia during 1982–2015. *Sci. Total. Environ.* **2019**, *653*, 1311–1325. [CrossRef]
68. Xu, L.; Tu, Z.; Zhou, Y.; Yu, G. Profiling Human-Induced Vegetation Change in the Horqin Sandy Land of China Using Time Series Datasets. *Sustainability* **2018**, *10*, 1068. [CrossRef]
69. Su, Y.; Li, X.; Feng, M.; Nian, Y.; Huang, L.; Xie, T.; Zhang, K.; Chen, F.; Huang, W.; Chen, J.; et al. High agricultural water consumption led to the continued shrinkage of the Aral Sea during 1992–2015. *Sci. Total. Environ.* **2021**, *777*, 145993. [CrossRef] [PubMed]
70. Huang, C.; Chen, Y.; Zhang, S.; Wu, J. Detecting, Extracting, and Monitoring Surface Water from Space Using Optical Sensors: A Review. *Rev. Geophys.* **2018**, *56*, 333–360. [CrossRef]
71. Pickens, A.H.; Hansen, M.C.; Hancher, M.; Stehman, S.V.; Tyukavina, A.; Potapov, P.; Marroquin, B.; Sherani, Z. Mapping and sampling to characterize global inland water dynamics from 1999 to 2018 with full Landsat time-series. *Remote Sens. Environ.* **2020**, *243*, 111792. [CrossRef]
72. Wang, J.; Song, C.; Reager, J.T.; Yao, F.; Famiglietti, J.S.; Sheng, Y.; Macdonald, G.M.; Brun, F.; Schmied, H.M.; Marston, R.A.; et al. Recent global decline in endorheic basin water storages. *Nat. Geosci.* **2019**, *11*, 926–932. [CrossRef]
73. Pan, N.; Wang, S.; Liu, Y.; Li, Y.; Xue, F.; Wei, F.; Yu, H.; Fu, B. Rapid increase of potential evapotranspiration weakens the effect of precipitation on aridity in global drylands. *J. Arid. Environ.* **2021**, *186*, 104414. [CrossRef]
74. van Beek, L.; Milkoreit, M.; Prokopy, L.; Reed, J.B.; Vervoort, J.; Wardekker, A.; Weiner, R. The effects of serious gaming on risk perceptions of climate tipping points. *Clim. Chang.* **2022**, *170*, 31. [CrossRef]
75. Oldfield, F.; Dearing, J.A. The Role of Human Activities in Past Environmental Change. In *Paleoclimate, Global Change and the Future*; Alverson, K.D., Pedersen, T.F., Bradley, R.S., Eds.; Global Change—The IGBP Series; Springer: Berlin/Heidelberg, Germany, 2003; pp. 143–162. [CrossRef]
76. Hornborg, A.; Crumley, C.L. (Eds.) *The World System and the Earth System: Global Socioenvironmental Change and Sustainability Since the Neolithic*, 1st ed.; Routledge: Abingdon, UK, 2006. [CrossRef]
77. Bernardino, P.N.; De Keersmaecker, W.; Fensholt, R.; Verbesselt, J.; Somers, B.; Horion, S. Global-scale characterization of turning points in arid and semi-arid ecosystem functioning. *Glob. Ecol. Biogeogr.* **2020**, *29*, 1230–1245. [CrossRef]
78. El-Wahab, R.H.A.; Al-Rashed, A.R.; Al-Dousari, A. Influences of Physiographic Factors, Vegetation Patterns and Human Impacts on Aeolian Landforms in Arid Environment. *Arid. Ecosyst.* **2018**, *8*, 97–110. [CrossRef]
79. Chen, H.; Liu, H.; Chen, X.; Qiao, Y. Analysis on impacts of hydro-climatic changes and human activities on available water changes in Central Asia. *Sci. Total. Environ.* **2020**, *737*, 139779. [CrossRef] [PubMed]
80. Wu, L.; Zhang, X.; Hao, F.; Wu, Y.; Li, C.; Xu, Y. Evaluating the contributions of climate change and human activities to runoff in typical semi-arid area, China. *J. Hydrol.* **2020**, *590*, 125555. [CrossRef]
81. Congalton, R.G.; Green, K. *Assessing the Accuracy of Remotely Sensed Data: Principles and Practices*; Lewis Publishers: Boca Raton, FL, USA, 1999.
82. Reinhart, V.; Fonte, C.; Hoffmann, P.; Bechtel, B.; Rechid, D.; Boehner, J. Comparison of ESA climate change initiative land cover to CORINE land cover over Eastern Europe and the Baltic States from a regional climate modeling perspective. *Int. J. Appl. Earth Obs. Geoinf.* **2021**, *94*, 102221. [CrossRef]
83. Wang, H.; Cai, L.; Wen, X.; Fan, D.; Wang, Y. Land cover change and multiple remotely sensed datasets consistency in China. *Ecosyst. Health Sustain.* **2022**, *8*, 2040385. [CrossRef]
84. ESA: Land Cover CCI Product User Guide Version 2.0, Tech. Report. 2017, p. 44. Available online: https://climate.esa.int/media/documents/CCI_Land_Cover_PUG_v2.0.pdf (accessed on 25 June 2022).